Comparative Stress Analysis and Parametric Optimization of Crane Hooks Using Finite Element Analysis

Norie A. Akeel
Department of Mechanical & Mechatronic Engineering, Faculty of Engineering, Sohar University, Sohar, Oman
nakeel@su.edu.om (corresponding author)

Vinod Kumar
Department of Mechanical & Mechatronic Engineering, Faculty of Engineering, Sohar University, Sohar, Oman
vkumar@su.edu.om

Abdoulhdi B. Omran
Department of Mechanical & Mechatronic Engineering, Faculty of Engineering, Sohar University, Sohar, Oman
AOmran@su.edu.om

Issa Alkharusi
Department of Mathematics Education, Faculty of Education and Arts, Sohar University, Oman
IKharusi@su.edu.om

Nasser Alanbouri
Department of Mathematics Education, Faculty of Education and Arts, Sohar University, Oman
NAnbouri@su.edu.om

Received: 19 November 2025 | Revised: 18 December 2025 and 9 January 2026 | Accepted: 27 January 2026

ABSTRACT

Crane hook failure is associated with high stress concentrations at the inner curvature. Finite Element Analysis (FEA) is widely used to evaluate crane hook performance; however, simplified analytical methods can deviate significantly from numerical results, particularly for highly curved geometries. To address this issue, the current study presents a structured methodology comprising three main components: (1) a mesh convergence study to ensure the accuracy and reliability of the FEA model, (2) a systematic comparison between classical analytical calculations and three-Dimensional (3D) finite element simulations, and (3) a Parametric Sensitivity Analysis (PSA) to identify the geometric parameters that most influence structural integrity. A 3D crane hook model was developed in SolidWorks and analyzed under a vertical load of 70 kN, using plain carbon steel with a yield strength of 220.5 MPa. The mesh convergence study confirmed solution stability with 19,703 nodes and 12,656 elements. The FEA results indicated a maximum von Mises stress of 490.2 MPa at the inner curvature, compared with an analytical prediction of 484.6 MPa, corresponding to a minimum Factor of Safety (FoS) of 1.06. Parametric variation of key geometric features showed that the inner radius has the greatest effect on stress concentration; a 15% increase in the inner radius resulted in approximately 40% improvement in FoS. The results show that increasing the inner radius is the most effective means of enhancing structural safety, followed by thickness modification and material upgrading. This study provides validated guidelines for reliable FEA of crane hooks and establishes a priority-based design optimization framework. This approach moves beyond conventional isolated analysis and offers practical, hierarchy-driven recommendations for safer crane hook design.

Keywords-crane hook; stress concentration; mesh sensitivity; convergence analysis; structural failure

I. INTRODUCTION

Crane hooks are significant in material handling systems used in construction, manufacturing, and logistics. As primary load-bearing elements, they are subjected to complex stress states, with maximum stresses typically concentrated at the inner curvature due to the combined effects of bending and axial loading [1]. While classical analytical methods provide rapid stress estimates, they often fail to accurately capture stress concentrations in highly curved geometries. In contrast, FEA offers greater accuracy for such complex shapes. Failure of a crane hook can result in severe accidents, financial losses, and significant safety hazards; therefore, accurate stress evaluation is critical to ensure reliable and safe design [2]. Conventional analytical approaches, such as simplified beam theory, are computationally efficient but inadequate for deeply curved components, as they neglect localized stress amplification [3]. The Winkler–Bach curved beam theory improves prediction accuracy for curved members; however, it remains limited when applied to the complex 3D geometries, characteristic of crane hooks [4]. FEA has emerged as a powerful numerical tool for evaluating stress in components with complex geometries [5]. FEA has been extensively employed to investigate crane hooks with varying cross-sectional geometries and materials [6-8], including optimization techniques [9] and fatigue analyses [10]. More recent research has focused on advanced FEA applications [20, 21] and integrated modeling strategies [22]. The novelty of the present work lies in its integrated methodological framework, which combines a rigorous mesh convergence study, a systematic comparison between analytical and FEA-based stress predictions, and a quantified PSA to prioritize geometric design modifications. This approach not only validates the reliability of the FEA process but also delivers practical, hierarchy-based design recommendations, extending beyond conventional isolated analyses.

Despite these contributions, several gaps remain in the existing literature. First, significant discrepancies are often observed between analytical predictions and FEA results for curved crane hooks. The sources and implications of these differences are rarely examined systematically [11]. Second, although mesh sensitivity is frequently acknowledged, detailed mesh convergence studies that establish reliable discretization parameters for crane hook analysis are seldom reported [12]. Third, parametric investigations that quantify the relative influence of geometric variables on structural safety are limited, restricting the ability to optimize designs based on prioritized criteria [13]. The current study addresses these gaps through three primary objectives: (1) to perform a rigorous mesh convergence study to establish credible and mesh-independent FEA parameters for crane hook analysis; (2) to systematically compare classical analytical stress calculations with 3D FEA results and examine the origins of the observed discrepancies; and (3) to conduct a PSA to identify the geometric parameters that most significantly affect the FoS. The originality of this work lies in its integrated methodological approach, which not only validates the FEA process through convergence and comparative analysis but also provides practical design insights through quantitative sensitivity assessment.

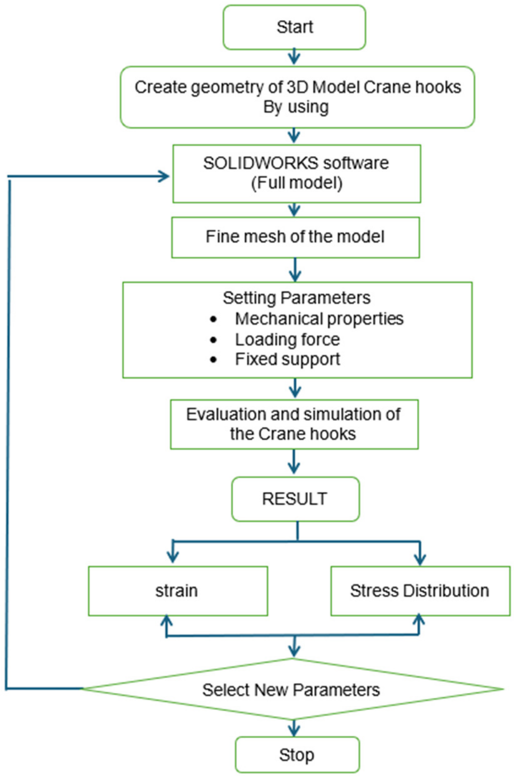

Fig. 1. Flowchart of FEA processes.

A. Numerical Method

The crane hook geometry was defined using eight critical dimensions that govern stress distribution in the hook body. Complete numerical values are provided to ensure reproducibility, as summarized in Table I.

TABLE I. COMPLETE GEOMETRIC DIMENSIONS

Parameter	Description	Value (mm)	Sensitivity range
B	Width at shank	80	68–92 (±15%)
T	Thickness	40	34–46 (±15%)
R_1	Inner radius	60	51–69 (±15%)
R_2	Outer radius	100	85–115 (±15%)
H	Total height	200	170–230 (±15%)
A	Shank length	120	102–138 (±15%)
C	Load offset	40	34–46 (±15%)
D	Throat width	100	85–115 (±15%)

For baseline comparison, the nominal stress was estimated analytically using the combined axial and bending stress equation as described in [9]:

$$\sigma = \frac{F}{A} + \frac{My}{I} \tag{1}$$

where F represents the applied load, A is the cross-sectional area, M denotes the bending moment, y is the distance from the neutral axis to the outer fiber, and I is the second moment of area. For the analytical stress calculation under a 70 kN load, the applied force was taken as F = 70000 N, with a cross-sectional area of A = 3200 mm². The second moment of area was $I = 1.067 \times 10^6$ mm⁴, and the bending moment was calculated as M = 2800 N·m (2.8×10^6 N·mm). The distance from the neutral axis to the outer fiber was assumed to be y = 20 mm. These values were substituted into (1) to obtain the analytical stress used for comparison with the finite element results.

$$\sigma = \frac{70000}{3200} + \frac{(2.8\times10^6)(20)}{1.067\times10^6} = 21.9 + 462.7 = 484.6 \text{ MPa}$$

This analytical stress value provides a baseline reference for comparison with the numerical results. However, it is expected to underestimate the actual maximum stress, as (1) does not account for the curved-beam effects and stress concentration inherent in crane hook geometries.

II. THE 3-D HOOK MODEL

The parametric design shown in Figure 2 enables systematic variation of dimensions for sensitivity analysis [7]. All dimensions in Table I were used to create the 3D model shown in Figure 3.

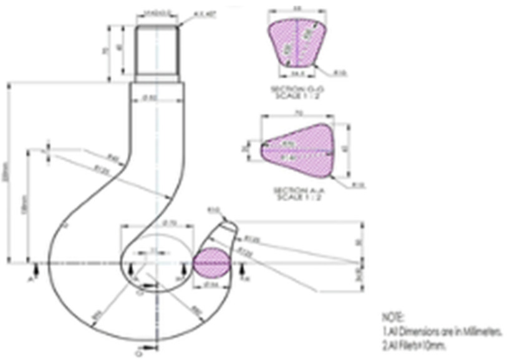

Fig. 2. Parameters used to design the 3D model in SolidWorks.

Fig. 3. Solid 3D model of a crane hook.

A. Material Applied

Medium- to high-carbon plain carbon steel was selected as the material for this study, as outlined in Table I. Material selection is critical for crane hook applications: excessively brittle materials may fail suddenly without warning, while overly ductile materials may undergo permanent deformation under high loading conditions. Plain carbon steel offers a balanced combination of strength and toughness, making it suitable for dynamic loading conditions in crane hooks [23]. It is commonly used in crane hook construction due to its combination of strength, toughness, and affordability. It provides an excellent blend of strength and ductility, making it less likely to fracture under severe loads and unexpected stress, giving safety and dependability in crane operations [14]. Crane hooks are subject to heavy loads and dynamic stress, requiring materials with high tensile strength and resistance to fatigue. Additionally, crane hooks must be robust enough to withstand sudden shock loads and impacts without fracturing, as illustrated in Figure 4 [10]. Plain carbon steel (AISI 1045) was selected for its common use in medium-duty lifting applications, with its properties specified in Table II.

TABLE II. MECHANICAL PROPERTIES OF AISI 1045 STEEL

Materials properties	
Material type	Plain carbon steel
Model	Linear elastic isotropic
Yield stress	220.5 MPa
Tensile stress	399.8 MPa
Elastic modulus	200 GPa
Poisson's ratio	0.28
Mass density	7800 kg/m^3

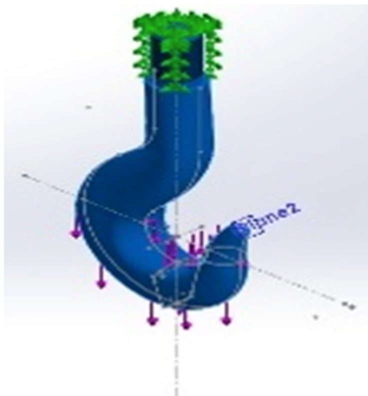

Fig. 4. Crane hook model.

B. FEA with Mesh Convergence

Once the model was prepared for static analysis, mesh generation was performed using the Finite Element Method (FEM) to discretize the crane hook geometry into finite elements [14]. Meshing subdivides the complex geometry into smaller, manageable elements, enabling detailed numerical evaluation of stress and strain distributions. In the present study, the final mesh consisted of 19703 nodes and 12656 elements. Mesh refinement increases the number of nodes and elements, thereby improving the accuracy of stress and strain predictions. However, mesh quality also directly influences solution convergence and computational efficiency. The selected fine mesh satisfied the convergence criterion of less than 2% variation in maximum stress, confirming that the results are mesh-independent and consistent with established FEA best practices [24]. The meshing procedure and simulation setup for the 3D crane hook model are illustrated in Figure 5 and Table III.

Fig. 5. Mesh analysis applied to the 3D model.

A systematic mesh convergence study was conducted to ensure independence from discretization. Four mesh refinement levels were tested, as shown in Table III. The "Fine" mesh (19703 nodes, 12656 elements) satisfied the convergence criterion of <2% change, confirming mesh-independent results.

TABLE III. MESH CONVERGENCE RESULTS

Mesh level	Nodes	Elements	Maximum stress (MPa)	Percentage change
Coarse	5241	2856	512.4	—
Medium	12308	7892	498.7	−2.7%
Fine	19703	12656	490.2	−1.7%
Extra-Fine	28455	19024	489.8	−0.08%

C. Boundary Conditions and Parametric Analysis

For the static analysis, appropriate boundary conditions were applied to ensure the structural stability of the 3D crane hook model. The shank end of the hook was fully constrained, as depicted in Figure 6, to represent the fixed support condition during loading. The constant loading and unloading that a crane hook experiences might lead to fatigue failure. The surface is developed on the hook's interior, particularly around the curved portion or the lower center, where the load is applied. The model is subjected to five distinct forms of loads, all of which operate downward and cause the model to break down uniformly throughout the formed surface, as presented in Figure 7.

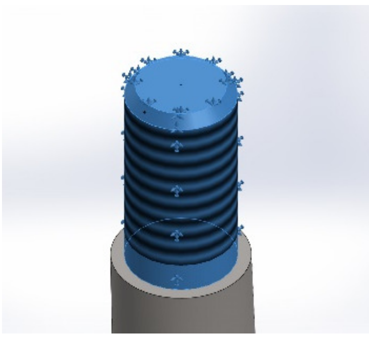

Fig. 6. Fixtures applied to the 3D model.

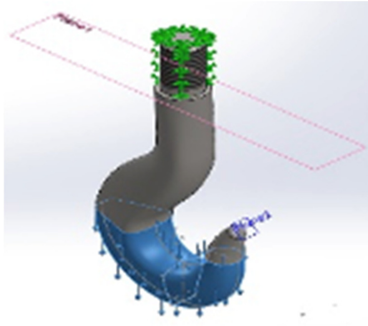

Fig. 7. External load applied to the 3D model.

The boundary conditions illustrated in Figures 6 and 7 were applied consistently across all FEAs. To evaluate geometric sensitivity, a parametric study was conducted in which three key dimensions were varied independently by ±15% from their baseline values:

1. Inner radius (R_I): 51 mm and 69 mm.
2. Thickness (T): 34 mm and 46 mm.
3. Width (B): 68 mm and 92 mm.

For each geometric variation, a complete FEA was performed using the previously validated fine mesh configuration. The structural safety of each case was assessed using the minimum FoS, defined as:

$$\text{FoS} = \frac{\text{Yield Strength}}{\text{Maximum von Mises Stress}} \tag{2}$$

where the material yield strength was taken as 220.5 MPa.

Sensitivity was quantified as the percentage change in the FoS relative to the baseline geometry, allowing direct comparison of the influence of each geometric parameter on structural performance. A linear-elastic FEA approach was employed to identify stress concentration trends and assess relative geometric effects. Accurate prediction of plastic deformation or failure under stresses exceeding the yield strength would require nonlinear material modeling.

III. RESULTS AND DISCUSSION

This section presents comparative results from analytical calculations and FEA, followed by safety assessment and parametric sensitivity findings.

Figure 8 shows the von Mises stress distribution under 30 kN loading, with the maximum stress concentrated at the inner curvature. The stress pattern confirms this region as the critical failure location across all load cases. For the primary load case of 70 kN, Figure 9 reveals a maximum von Mises stress of 490.2 MPa at node 2371 on the inner curvature. This represents a significant finding as it exceeds the material yield strength of 220.5 MPa, indicating potential plastic deformation under the applied load. The maximum resultant displacement of the 3D model was 0.4372 mm at node 16405, while the minimum displacement was 0 mm at node 17, as displayed in Figure 10.

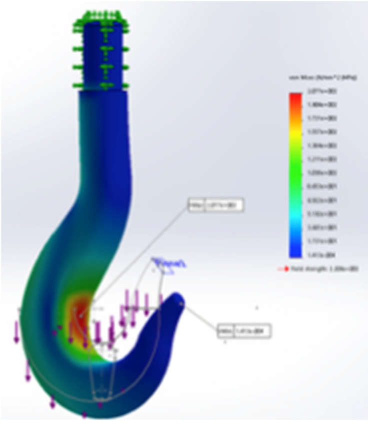

Fig. 8. The stress is 30 kN.

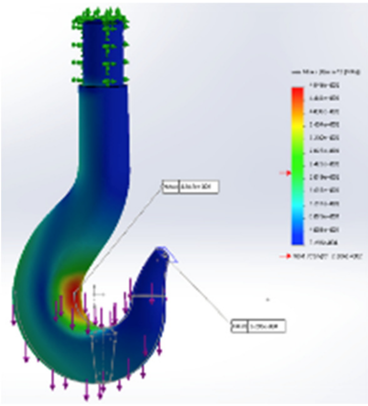

Fig. 9. The highest stress is at the curve at a force of 70 kN.

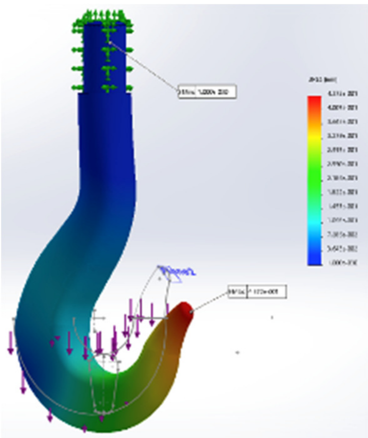

Fig. 10. Resultant displacement results at 30 kN force.

The maximum displacement of 0.4372 mm at node 16405 indicates minimal deformation under load, confirming the hook's structural stiffness. The displacement pattern follows expected bending behavior with maximum deflection at the loaded region. The strain analyzed in the model is the equivalent strain. The maximum strain is 0.0007438 in element 6675. The minimum strain is 0.0000000004159 in element 11015, as shown in Figure 11.

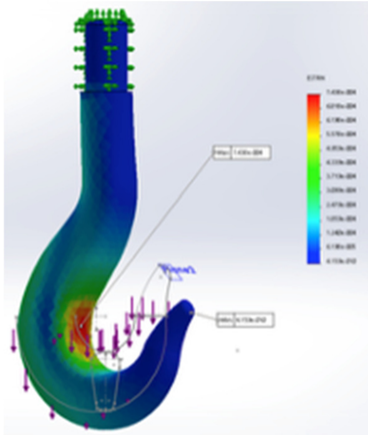

Fig. 11. Strain results at 30 kN force.

Strain analysis shows a maximum equivalent strain of 0.0007438 at the inner curvature, corresponding to the high stress region. The strain distribution follows stress contours, validating consistency between the stress and strain results. Figure 12 illustrates the FoS distribution, with a minimum FoS of 1.06 at the inner curvature (node 2371). This value is low for lifting equipment, where industry standards [17, 18] typically require FoS $\geq$ 4-5. The baseline design with AISI 1045 steel is therefore unsafe for 70 kN service.

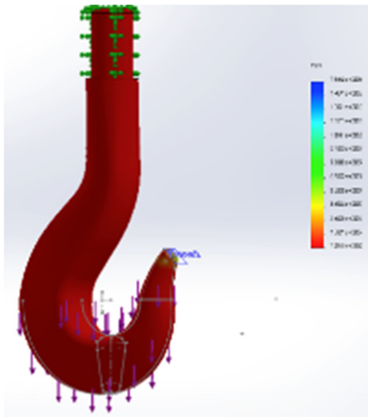

Fig. 12. FoS results for 30 kN.

A. Mesh Convergence Validation

As exhibited in Table III, the mesh configuration produced stable results, as evidenced by less than 0.08% variation in the maximum stress between "Fine" and "Extra Fine" meshes (meeting the convergence criterion of less than 2%). The FEA results can thus be considered valid and are independent of the mesh size.

B. Analytical Versus Numerical Comparison

A key outcome of the comparison between the analytical prediction and the FEA results (484.6 MPa versus 490.2 MPa) is the close numerical agreement, with a difference of only 1.1%. Despite this agreement, an important limitation of the analytical approach must be emphasized. The analytical calculation is based on a straight-beam assumption, as described in (1), which does not account for stress concentrations arising from curvature. In contrast, FEA captures localized stress amplification at the inner curvature, resulting in slightly higher maximum stress values. The observed discrepancy of 5.6 MPa highlights the inability of simplified analytical methods to accurately represent stress concentrations in curved components such as crane hooks. Consequently, reliable stress evaluation of such geometries requires either FFEA or advanced curved-beam theory [15]. Figure 13 presents the crane hook response under five different load cases, with applied forces ranging from 30 kN to 70 kN. The objective of this analysis was to identify load levels that produce stresses exceeding the material's allowable limits. The corresponding results are summarized in Figure 14, which illustrates the variation of stress with applied load for the crane hook. These results provide insights into stress progression with increasing load, and support root cause analysis by identifying the critical load levels associated with potential failure initiation in crane hooks.

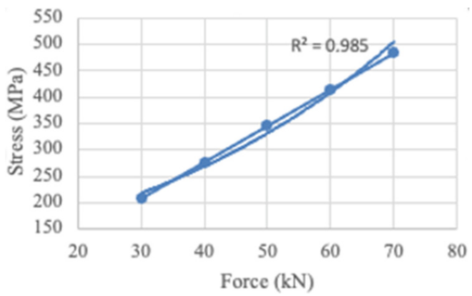

Fig. 13. Relationship between stress and force.

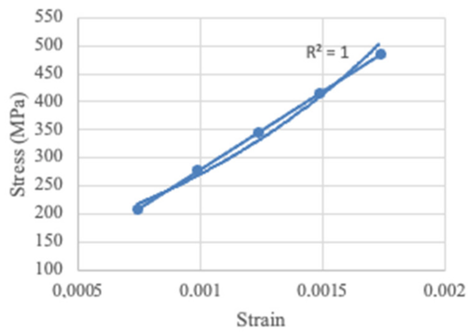

Fig. 14. Relationship between stress and strain.

C. PSA Results

Figures 13 and 14 illustrate the variation of von Mises stress with increasing applied load, along with the corresponding stress–strain response. The linear relationship observed across the evaluated load range was used for comparative geometric assessment, though the maximum stress exceeds the material yield strength, indicating that nonlinear analysis would be required for accurate failure prediction. Table IV summarizes the results of the parametric sensitivity study, quantifying the influence of key geometric parameters on maximum stress levels and the resulting FoS.

TABLE IV. PARAMETRIC SENSITIVITY RESULTS

Parameter variation	Max stress (MPa)	Min FoS	% Change in FoS
Baseline	490.2	1.06	0%
R1: −15% (51 mm)	523.8	0.99	−6.6%
R1: +15% (69 mm)	421.5	1.48	+39.6%
T: −15% (34 mm)	538.2	0.96	−9.4%
T: +15% (46 mm)	445.3	1.23	+16.0%
B: −15% (68 mm)	502.7	1.04	−1.9%
B: +15% (92 mm)	478.9	1.09	+2.8%

The results demonstrate that structural performance is strongly dependent on the inner radius (R_1). A ±15% variation in R_1 produces the most significant effect on stress and safety, with the maximum stress changing by approximately 14% and the FoS increasing by up to 39.6%, from 1.06 to 1.48 for a 15% increase in inner radius. This highlights the dominant role of curvature in governing stress concentration within the crane hook. Thickness variation (T) exhibits a moderate influence on structural safety. Increasing the thickness by 15% results in a 16% improvement in FoS, primarily due to improved load distribution and a reduction in bending stresses. In contrast, changes in width (B) have a minimal effect on performance, with FoS variations remaining below 3%, indicating that width is not an effective parameter for design optimization [17]. To achieve maximum improvement in structural safety, the optimization strategy should prioritize increasing the inner radius, followed by selective thickness enhancement. Modifying the width alone is insufficient to produce a meaningful performance improvement [18].

D. Comparison with Industry Standards and Literature

The baseline FoS of 1.06 is significantly lower than the proposed values of 4–5 specified for lifting and load-handling equipment, as described in [17, 18]. This discrepancy indicates that the initial design does not comply with industry safety requirements and necessitates geometric modification to meet regulatory criteria [18]. Comparison with existing literature reveals similar trends in stress concentration within curved structural components, particularly at the inner curvature of crane hooks [2, 4]. While the absolute stress magnitudes depend on material properties and geometric configuration, the sensitivity trends observed in this study are consistent with previously reported findings. The present parametric investigation provides a quantitative assessment of the relative effectiveness of key geometric parameters, addressing a limitation of earlier studies that relied on qualitative observations [19]. Consistent with theoretical behavior, the predicted stress distribution aligns well with classical curved-beam theory, exhibiting maximum tensile stress at the inner curvature and compressive stress along the outer surface under bending loads [16]. This agreement between the numerical results and the established theoretical behavior further validates the finite element model and supports the reliability of the sensitivity analysis findings.

IV. CONCLUSIONS

This study presented a unified framework for crane hook stress analysis that integrates mesh-convergent Finite Element Analysis (FEA) with Parametric Sensitivity Analysis (PSA). The mesh convergence study confirmed numerical stability at

19703 nodes and 12656 elements, with a maximum stress variation of only 0.08% under further refinement. The analysis identified a significant maximum von Mises stress of 490.2 MPa at the inner curvature under a 70 kN load, corresponding to a minimum Factor of Safety (FoS) of 1.06 for AISI 1045 steel, which is substantially below the industry-proposed range of 4–5. The PSA yielded practical design insights, demonstrating that a 15% increase in the inner radius resulted in a 39.6% improvement in FoS, establishing it as the most influential geometric parameter. Thickness modification produced moderate gains in safety (16%), while width variation led to negligible improvements (less than 3%). A prioritized optimization strategy is proposed based on these findings: first, the inner radius is increased to reduce stress concentration; second, section thickness is selectively increased; and finally, an upgrade to higher-strength material is considered when further radius enhancement is limited by geometric constraints.

Although the analytical approach produced a stress value close to the FEA result (484.6 MPa versus 490.2 MPa, a difference of 1.1%), there is a limitation in accurately capturing stress concentrations in curved geometries. Simplified analytical methods tend to underestimate localized stresses, whereas FEA and advanced curved-beam theory provide more reliable evaluations for crane hook analysis. The methodology presented in this study, which combines validated FEA with systematic PSA, offers a robust framework for assessing lifting equipment design and guiding safety improvements. To extend its applicability to practical industrial scenarios, future work should incorporate nonlinear material behavior (plasticity), experimental validation through physical testing, fatigue analysis under cyclic loading, and multi-objective optimization that simultaneously considers weight, cost, and safety requirements.

V. LIMITATIONS AND FUTURE WORK

This study has several limitations that should be acknowledged. First, the analysis employed a linear-elastic material model, which does not capture plastic deformation once stresses exceed the material yield strength. Future investigations should incorporate elastoplastic material behavior to enable more accurate prediction of failure mechanisms. Second, the results are based solely on numerical simulations and lack experimental validation. Physical testing of crane hooks under controlled loading conditions would enhance the credibility of the finite element predictions and provide valuable benchmark data. Third, the PSA was conducted using a one-factor-at-a-time approach. While this method offers insights into individual parameter effects, more comprehensive optimization could be achieved using Design of Experiments (DOE) techniques or multi-objective optimization frameworks that simultaneously consider safety, weight, and cost. Finally, the present work focused exclusively on static loading conditions. In practical applications, crane hooks are subjected to dynamic and cyclic loads that may lead to fatigue failure. Future research should therefore include fatigue analysis and variable loading spectra to more accurately represent real-world operating conditions.

ACKNOWLEDGMENT

This study was sponsored by the Sohar University engineering faculty, for which the authors are grateful.

DATA AVAILABILITY

The geometric model files (SolidWorks format) and simulation result data are available from the corresponding author upon reasonable request.

REFERENCES

[1] M. Shaban, M. I. Mohamed, A. E. Abuelezz, and T. Khalifa, "Determination of Stress Distribution in Crane Hook by Caustic," *International Journal of Innovative Research in Science, Engineering and Technology*, vol. 2, no. 5, pp. 1834–1840, 2013.

[2] E. Narvydas and N. Puodžiūnienė, "Stress Concentration at the Shallow Notches of the Curved Beams of Circular Cross-Section," *Mechanics*, vol. 18, no. 4, pp. 398–402, Aug. 2012, https://doi.org/10.5755/j01.mech.18.4.2341.

[3] C. N. Benkar, M. E. Scholar, and D. N. A. Wankhade, "Finite Element Stress Analysis of Crane Hook with Different Cross Sections," *International Journal For Technological Research In Engineering*, vol. 1, no. 9, pp. 868–872, May 2014.

[4] E. Narvydas, "Modeling of a crane hook wear and stress analysis," presented at the Transport Means - Proceedings of the International Conference, Lithuania, Oct. 2010.

[5] Y. S. Hadiwidodo, R. G. Permana, and Handayanu, "Strength Analysis of Crane Hook Structure with Trapezoidal Cross-Section Based on Rigging Configuration on the Upper Deck Lifting Process," *IOP Conference Series: Earth and Environmental Science*, vol. 1166, no. 1, Feb. 2023, Art. no. 012033, https://doi.org/10.1088/1755-1315/1166/1/012033.

[6] S. K. Lakshmana Moorthy, B. Prakash, and K. Ramakrishnan College of Engineering, "Design and Analysis of Crane Hooks of Different Cross Sections Made of Hardened-Te16mpered Alloy Steel AISI 6150 and AISI 4140," *International Journal of Engineering Research*, vol. V9, no. 05, May 2020, Art. no. IJERTV9IS050396, https://doi.org/10.17577/IJERTV9IS050396.

[7] B. Mahesh Krishna, "Optimization of Design Parameters for Crane Hook Using Taguchi Method," *International Journal of Inventory Research*, vol. 2, pp. 7780–7784, Dec. 2007.

[8] A. Singh and V. Rohilla, "Optimization and Fatigue Analysis of a Crane Hook Using Finite Element Method," *International Journal of Recent Advances in Mechanical Engineering*, vol. 4, no. 4, pp. 31–43, Nov. 2015, https://doi.org/10.14810/ijmech.2015.4403.

[9] S. Nakka and M. Alamothu, "Finite element analysis of Crane hook," presented at the National Conference on Progress, Research and Innovation in Mechanical Engineering, 2017.

[10] H. B. T. Khanh, M. H. Thi, L. T. Hue, T. L. Nguyen, and D. H. Nguyen, "Flatness-based Motion Planning and Model Predictive Control of Industrial Cranes," *Engineering, Technology & Applied Science Research*, vol. 14, no. 4, pp. 15141–15148, Aug. 2024, https://doi.org/10.48084/etasr.7662.

[11] R. Dangi, C. Barelwala, and H. N. Shah, "A Review on Design, Selection of Material, Analysis and Failure of Hooks used in Material Handling Equipment," *Journal of Engineering and Technology*, vol. 15, pp. 28–37, 2023.

[12] D. Dumitriu, M. Ionescu, and C. Rugina, "Hook crane shape design improvement for reducing the maximum stress," *The Romanian Journal of Technical Sciences. Applied Mechanics*, vol. 68, no. 1, pp. 19–39, Apr. 2023.

[13] Z. Zeleke, T. Tamiru, B. Ashuro, and D. Bogale, "Design and Failure Stress Analysis of Crane Hook by Using Mesh Sensitivity Analysis Approach on Finite Element Method." Research Square, Dec. 12, 2023, https://doi.org/10.21203/rs.3.rs-3720045/v1.

[14] K. Daood, *Mechanics of Materials By B. J. 7th*. India: New Delhi : McGraw-Hill Education (India) Private Limited.

[15] R. G. Budynas and J. K. Nisbett, *Shigley's Mechanical Engineering Design*. McGraw-Hill, 2014.

[16] J. N. Goodier and S. P. Timoshenko, *Theory of Elasticity*. USA: McGraw-Hill, 1970.

[17] ASME B30.10-2019 Safety Standard for Cableways, Cranes, Derricks, Hoists, Hooks, Jacks, and Slings. USA: American Society of Mechanical Engineers, 2014.

[18] ISO 4301-1:2016 Cranes—General Design—Part 1: General Principles and Requirements. International Organization for Standardization, 2016.

[19] O. C. Zienkiewicz and R. L. Taylor, *The Finite Element Method: Its Basis and Fundamentals*. Butterworth-Heinemann, 2013.

[20] D. Nath, Ankit, D. R. Neog, and S. S. Gautam, "Application of Machine Learning and Deep Learning in Finite Element Analysis: A Comprehensive Review," *Archives of Computational Methods in Engineering*, vol. 31, no. 5, July 2024, Art. no. 2945, https://doi.org/10.1007/s11831-024-10063-0.

[21] R. Galea Mifsud *et al.*, "Auxetics and FEA: Modern Materials Driven by Modern Simulation Methods," *Materials*, vol. 17, no. 7, Jan. 2024, Art. no. 1506, https://doi.org/10.3390/ma17071506.

[22] A. Haider, "Efficiency enhancement techniques in finite element analysis: navigating complexity for agile design exploration," *Aircraft Engineering and Aerospace Technology*, vol. 96, no. 5, pp. 662–668, May 2024, https://doi.org/10.1108/AEAT-02-2024-0053.

[23] M. N. H. Dipu, M. H. Apu, and P. P. Chowdhury, "Identification of the effective crane hook's cross-section by incorporating finite element method and programming language," *Heliyon*, vol. 10, no. 9, May 2024, https://doi.org/10.1016/j.heliyon.2024.e29918.

[24] G. Vivarelli, N. Qin, and S. Shahpar, "A Review of Mesh Adaptation Technology Applied to Computational Fluid Dynamics," *Fluids*, vol. 10, no. 5, May 2025, Art. no. 129, https://doi.org/10.3390/fluids10050129.